

Efficient visible light sensitisation of water-soluble near-infrared luminescent lanthanide complexes

2 PERKIN

Martinus H. V. Werts,^a Jan W. Verhoeven^{*a} and Johannes W. Hofstraat^b

^a Laboratory of Organic Chemistry, University of Amsterdam, Nieuwe Achtergracht 129, NL-1018 WS Amsterdam, The Netherlands

^b Philips Research Laboratories, Department of Polymers and Organic Chemistry, Prof. Holstlaan 4, NL-5656 AA Eindhoven, The Netherlands

Received (in Cambridge, UK) 8th December 1999, Accepted 4th January 2000

Fluorexon (4',5'-bis[*N,N*-bis(carboxymethyl)aminomethyl]fluorescein) forms stable, water-soluble complexes with lanthanide ions. The complexes with neodymium(III), erbium(III) and ytterbium(III) display sensitised near-infrared lanthanide luminescence upon excitation of the fluorexon with visible light. The photosensitisation efficiency is very high (0.5–1.0) as a result of lanthanide-enhanced intersystem crossing in the sensitising chromophore and rapid intracomplex energy transfer. The overall luminescence quantum yields, however, are low (2×10^{-4} – 5×10^{-3}) due to nonradiative deactivation of the excited lanthanide ion.

Introduction

Europium(III) and terbium(III) complexes that luminesce in the visible and contain organic chromophores as photosensitisers are already applied as labels for marking molecules of biological interest, e.g. in fluoroimmunoassays^{1–5} and in fluorescence microscopy.^{6,7} The incentive for the use of these labels instead of “conventional” fluorophores is that their long luminescence lifetimes (milliseconds) can be used to discriminate the label emission from the short-lived (nanoseconds) autofluorescence of the biological matrix. Using time-gated detection, i.e. exciting the sample with a short light pulse and only detecting the photons emitted at times later than a few microseconds, the autofluorescence and other interferences are effectively suppressed leaving only the lanthanide labels to be detected. This has been convincingly demonstrated by De Haas *et al.*, who combined biochemical (peroxidase mediated) signal amplification with time-delayed detection of Eu^{3+} -chelate labelled streptavidin and were able to observe the label luminescence by eye through a modified fluorescence microscope using delayed detection.⁷

In typical luminescent lanthanide complexes, population of the luminescent (lanthanide centered) state is achieved by energy transfer from a triplet excited organic chromophore.^{8,9} This indirect path, which involves the efficient excitation of the chromophore into its singlet state followed by intersystem crossing, is necessary since direct excitation of the lanthanide ion is difficult. Its intraconfigurational *f*–*f* transitions are only weakly allowed,¹⁰ which on the one hand gives rise to the long luminescence lifetimes, but on the other introduces the need for excitation *via* organic “antenna” chromophores. Here lies also the cause of one of the drawbacks of Eu^{3+} and Tb^{3+} based labels. The luminescence of these ions being in the visible, sensitisation of that luminescence through organic chromophores can only be effective if these have their lowest singlet transitions in the near-UV,¹¹ although we have recently shown that efficient sensitisation of Eu^{3+} luminescence for blue light excitation is possible under certain conditions.¹²

One might expect that if lanthanide ions with lower lying luminescent states are used, the absorption bands of the antenna chromophores can be pushed more towards the red. Recently, we studied¹³ complexes of neodymium(III),

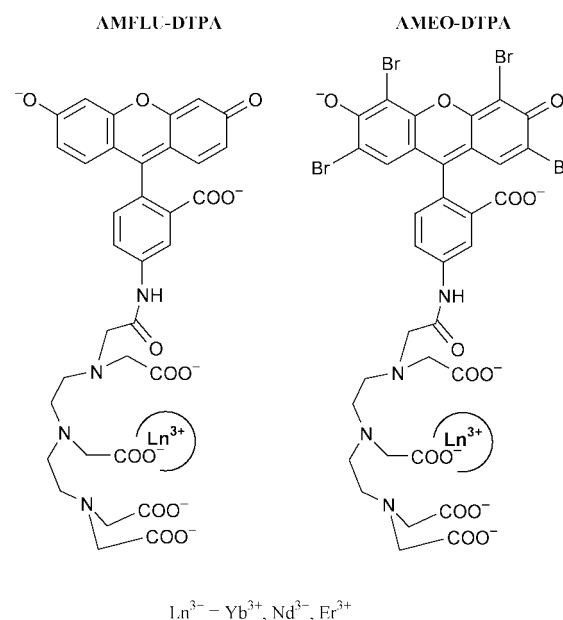


Fig. 1 Molecular structures of the $\text{Ln}(\text{AMFLU-DTPA})$ and $\text{Ln}(\text{AMEO-DTPA})$ complexes studied previously.¹³

erbium(III) and ytterbium(III) containing fluorescein and eosin as sensitising chromophores ($\text{Ln}(\text{AMFLU-DTPA})$ and $\text{Ln}(\text{AMEO-DTPA})$, see Fig. 1). These chelates already showed sensitised near-infrared luminescence from all three lanthanide ions upon excitation of the chromophore with visible light, and were the first near-infrared luminescent complexes in which ion and sensitiser had been brought together in a well-defined one-on-one way. In fact, the complexes of AMEO-DTPA and AMFLU-DTPA with Er^{3+} were the first examples of their kind to show Er^{3+} luminescence in solution. However, it soon became clear that in these complexes the energy transfer from the chromophores to the ions is not rapid enough. Dissolved molecular oxygen can compete well with the lanthanide ion as an alternative acceptor of the triplet energy of the chromophore, judging from the presence of $^1\text{O}_2$ ($^1\Delta_g \rightarrow ^3\Sigma_g$) phosphorescence at 1276 nm and the increase of lanthanide luminescence

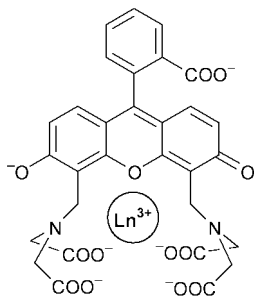


Fig. 2 Molecular structure of the Ln(fx) complex.

quantum yield upon deoxygenation. Also, a more detailed study showed that, as a result of incomplete intersystem crossing, a considerable amount of the excitation energy is lost due to fluorescence of the antenna chromophore, especially in the fluorescein containing complexes.^{14,15}

The actual chromophore of fluorescein, eosin and other xanthene dyes is the annelated three-ring system. The phenyl ring has been calculated to be almost perpendicular to this system.¹⁶ In fact, dyes lacking this group have recently been synthesised and show virtually the same photophysical parameters as the original dyes.^{17,18} Looking again at the molecular structures of the AMEO-DTPA and AMFLU-DTPA, we concluded that the phenyl ring might act as a spacer between the chromophore and the lanthanide ion, increasing the distance between the two and thereby reducing two interactions crucial to the efficiency of sensitisation. Firstly, the paramagnetic and heavy atom effects¹⁹ of the ion on the chromophore are diminished. These effects enhance intersystem crossing, favouring generation of sensitising triplets over emission of antenna fluorescence. Secondly, the exchange interaction between the electronic system of chromophore and that of the lanthanide ion is weakened, which is detrimental to the efficiency of (Dexter type) excitation energy transfer.

We therefore decided to investigate complexes of Yb³⁺, Nd³⁺ and Er³⁺ with 4',5'-bis[*N,N*-bis(carboxymethyl)aminomethyl]-fluorescein or fluorexon (Fig. 2).† The binding site of the lanthanide ion in these complexes should be much closer to the chromophore than in the AMFLU-DTPA and AMEO-DTPA complexes studied earlier. It is anticipated that if effective complexation with the lanthanide ions occurs the sensitisation efficiency will be higher.

In this paper, we will demonstrate that fluorexon, fx, indeed forms water-soluble 1 : 1 complexes with lanthanide ions, having a stability comparable to that of lanthanide ion–EDTA complexes. In complexes of fx with Nd³⁺, Er³⁺ and Yb³⁺, highly efficient population of the lanthanide ions' excited states is achieved *via* excitation of the fx chromophore. We will show that this is a result of both enhanced intersystem crossing in the antenna chromophore and rapid intracomplex energy transfer.

Experimental

Chemicals and solutions

Fluorexon (4',5'-bis[*N,N*-bis(carboxymethyl)aminomethyl]-fluorescein) was obtained from both Molecular Probes Europe (Leyden, The Netherlands) and Fluka. Ethylenediaminetetraacetic acid (EDTA), ordinary and perdeuterated Tris (tris-(hydroxymethyl)aminomethane), deuterium oxide, deuterium chloride (37 wt% in D₂O) and all lanthanide chlorides (as the hexahydrates) were purchased from Aldrich. Stock solutions (10⁻³–10⁻⁴ M) of fluorexon (in 0.1 M Tris–HCl buffer, pH 8.3)

† We refer here to the pure 4',5' isomer instead of the "indicator grade" fluorexon/calcein which is a mixture of isomers whose iminodiacetic acid groups are attached to the fluorescein chromophore at different positions.

and lanthanide chlorides (in 0.5 M HCl) were freshly prepared before each experiment and diluted where appropriate. Unless otherwise indicated measurements were done on complexes in aerated 0.1 M Tris–HCl buffer (pH 8.3). The complexes were prepared by mixing equal amounts of equimolar solutions (10⁻⁵–10⁻⁶ M) of ligand and lanthanide ion. The resulting solutions were heated briefly and then allowed to equilibrate for three hours at room temperature.

UV–Vis spectroscopy

UV–Vis absorbance spectra were recorded on a Cary 3, a Cary 3E or a Hewlett Packard 8543 diode array spectrophotometer.

Steady-state luminescence spectroscopy

Two set-ups were used for luminescence spectroscopy in the visible and the near-infrared. The Spex Fluorlog 3–22 instrument delivers the excitation light from a 450 W Xe lamp *via* a double grating monochromator to the sample. For spectroscopy in the 300–900 nm emission range, the emission light is collected at right angles by a double grating monochromator and detected by a Peltier cooled R636-10 (Hamamatsu) photomultiplier operating in photon counting mode. Alternatively, emission in the range 400–1100 nm is analysed and detected in this set-up by a Princeton Instruments Peltier cooled CCD camera (TEA/CCD-1024-EM1) combined with an Acton spectrograph (SpectraPro 150). The latter combination can readily detect the 880 nm Nd³⁺ and 980 nm Yb³⁺ emission of the complexes of these ions in water.

The other instrument is a modified PTI Alphascan fluorimeter, in which the light from a 75 W quartz–tungsten–halogen lamp is focused into a Spex 1680 double monochromator and subsequently onto the sample. Emission in the visible is detected under right angle by a R928 (Hamamatsu) photomultiplier after dispersion by a PTI 0.25 m single monochromator. Detection in the near-infrared (900–1600 nm) is achieved by modulating the excitation light with a mechanical chopper (at 35–70 Hz), passing the emitted light through a similar PTI single monochromator and focusing it onto a liquid nitrogen cooled germanium detector (North Coast 817L) connected to a Stanford Research SRS530 lock-in amplifier which detects the modulated signal.

Where necessary filters were used to remove scattered excitation light and second order emission light. Excitation spectra were corrected for differences in excitation intensity, emission spectra were corrected for the wavelength dependence of the detection efficiency. All spectra are reported in relative numbers of quanta per unit wavelength.

Time resolved near-infrared luminescence measurements

The set-up for time-resolved near-infrared luminescence consists of a nitrogen laser (Laser Technik Berlin MSG405-TD, 337 nm pulses of 500 ps FWHM) as the excitation source, and an Edinburgh Instruments single monochromator and a North Coast liquid nitrogen cooled germanium detector for spectral and temporal resolution of the luminescence. The time response of this system is approx. 400 ns FWHM and is entirely determined by the response of the Ge detector. The signal was recorded by a Tektronix digitising oscilloscope and its digital representation was transferred to a microcomputer for analysis.

The luminescence decay times of the complexes being of the same order of magnitude as the instrumental response, it is often necessary to deconvolute the measured time traces to obtain reliable luminescence kinetics, as has already been demonstrated^{20,21} by Beeby *et al.* for Nd³⁺ and Yb³⁺ complexes. To this end, the instrument response was obtained by recording the signal of a solution of the near-infrared fluorescent dye IR 140 in ethanol. Its fluorescence lifetime is less than 1 ns, which is much shorter than the instrumental response. Therefore, the

measured signal will faithfully represent this response. Actual deconvolution was achieved by numerical iterative reconvolution on a microcomputer. Two programs were used: a commercial program (Edinburgh Instruments) available on the experimental set-up, and a home written program. The latter was programmed in Igor Pro 3.1 (Wavemetrics, Inc., Lake Oswego, Oregon, USA), and uses a simplex algorithm instead of Levenberg–Marquardt to minimise the χ^2 . The results of both programs are evidently the same, but the more flexible nature of the home written program allows us to conveniently test and compare different kinetic schemes to describe the luminescence.

Transient absorption measurements

Transient absorption spectra were measured by pumping the sample with pulses of less than 2 mJ at 308 nm from a Lumonics XeCl excimer laser and probing the sample perpendicular to the excitation with an EG&G Xe flash lamp (FX504) and a spectrograph (Acton Spectrapro-150) coupled to an intensified CCD camera (Princeton Instruments ICCD-576-G/RB-EM). The excited state was probed by opening the gate of the detector during 10 ns, 100 ns after the laser pulse. The time-dependent behaviour of excited species was monitored in a separate experiment with a non-pulsed Xe arc, a Zeiss prism monochromator and a photomultiplier (1P28, S5 photocathode) coupled to a Tektronix TDS684B oscilloscope as the probe system, and the same laser as the excitation source.

Fluorimetric titrations

For the determination of the preferred ion–ligand stoichiometry, the equimolar solutions were mixed in different ratios and submitted to the same equilibration procedure as mentioned above. The samples were excited at 480 nm, and the spectrum of the main luminescent transition of the respective lanthanide ion was recorded: the region around 980 nm for Yb^{3+} , around 1530 nm for Er^{3+} and around 1060 nm for Nd^{3+} . The emission bands were integrated to yield the total luminescence intensity. Also the antenna fluorescence band (500–700 nm) was recorded and integrated. The spectrograph/CCD combination was particularly convenient in this respect, since—with the proper optical filtering—it enables simultaneous recording of the tail of the antenna fluorescence band and the Nd^{3+} and Yb^{3+} emission bands.

Near-infrared luminescence quantum yield measurements

The near-infrared quantum yields of the Nd^{3+} and Yb^{3+} complexes were measured relative to $\text{Ru}(\text{bpy})_3^{2+}$ in deoxygenated water²² ($\Phi_{\text{lum}} = 0.042$ at 293 K) using the spectrograph/CCD combination following well-known procedures.^{23,24} The emission spectra were corrected using factors obtained by measuring the emission of a calibrated lamp (EG&G Gamma Scientific RS10A lamp with RS3 power supply). The validity of the correction factors was checked by comparing the corrected recorded spectrum and the measured quantum yield of cresyl violet with the data published by Magde *et al.*²⁵ All values agreed within 5%. The quantum yield of the Er^{3+} complex was determined relative to $\text{Yb}(\text{fx})$ and $\text{Nd}(\text{fx})$ using the corrected emission spectra of the complexes recorded using the Ge-detector.

Results and discussion

Nature of the complex

Addition of Yb^{3+} ions to a solution of fx changes the absorption spectrum and quenches the fluorescence of fx. Together with the observation of Yb^{3+} luminescence ($\lambda \approx 980$ nm) upon excitation of fx, these effects clearly indicate the formation of luminescent complexes between Yb^{3+} and fx. Before under-

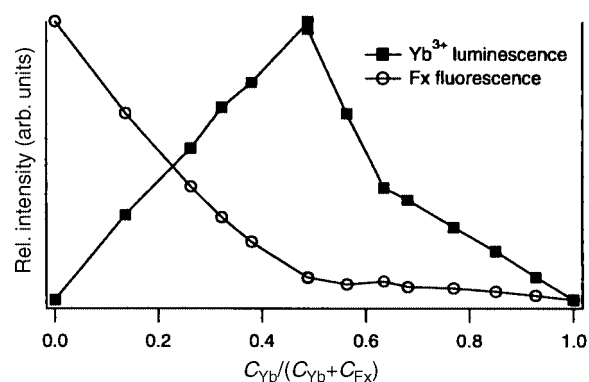


Fig. 3 Job plot of the complex formation of Yb^{3+} with fluorexon, monitored with luminescence spectroscopy. $c_{\text{Yb}} + c_{\text{Fx}}$ was held at 1.1×10^{-5} M in 0.1 M Tris–HCl (pH 8.3). The sample was excited at 480 nm.

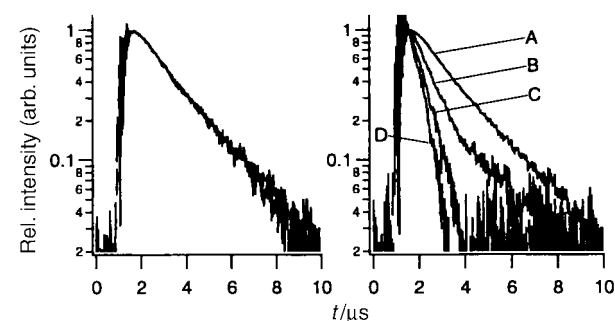


Fig. 4 NIR luminescence decay curves of solutions of Yb^{3+} and fx in Tris–HCl buffer monitored at 980 nm under excitation with 337 nm pulses. Left: Overlaid decays of the samples having $c_{\text{Yb}}/c_{\text{Fx}} \leq 1$ (Yb^{3+}/fx ratios 1:4, 1:2, 2:3 and 1:1). Right: Decays of the samples having $c_{\text{Yb}}/c_{\text{Fx}} \geq 1$. Yb^{3+}/fx ratios (A) 1:1, (B) 3:2, (C) 2:1 and (D) 4:1.

taking a study of the photophysical properties of such complexes, it is necessary to find out what kind of complexes will be dealt with. The EDTA-like structure of the chelating part of the molecule, combined with simple electrostatic considerations, suggest that a 1:1 complex is most likely, but other types of complexes cannot be ruled out beforehand. Varying both the total added concentration of Yb^{3+} (c_{Yb}) and that of fluorexon (c_{Fx}), the complex formation between the two was investigated.

Insight into the preferred stoichiometry is provided by an experiment in which the total concentration of Yb^{3+} and fx is held fixed ($c_{\text{Yb}} + c_{\text{Fx}} = 1.1 \times 10^{-5}$ M), varying the ratio of the components ($c_{\text{Yb}}/c_{\text{Fx}}$). This is achieved by mixing equimolar solutions (1.1×10^{-5} M) of the components, heating the solutions briefly using a hot air gun, and letting them cool down to room temperature. At $c_{\text{Yb}}/c_{\text{Fx}} = 1$ the luminescence intensity (upon excitation of the ligand at 470 nm) is maximised (Fig. 3). In the region $c_{\text{Yb}}/c_{\text{Fx}} \leq 1$ this intensity is linearly correlated with the concentration of Yb^{3+} , and so is the quenching of the fluorexon fluorescence (Fig. 3). Evidently, under these conditions 1:1 complex formation takes place. The linearity is lost when $c_{\text{Yb}}/c_{\text{Fx}} \geq 1$, indicating the formation of other species.

Time-resolved measurements of the near-infrared Yb^{3+} luminescence yield monoexponential decays for the samples with $c_{\text{Yb}}/c_{\text{Fx}} \leq 1$ ($\tau = 1.9$ μs , Fig. 4 left), strengthening our idea that under these conditions only one luminescent species, the 1:1 complex, is present. The formation of multiple species in the case of excess Yb^{3+} is apparent from the multi-exponential behaviour of the luminescence decays observed from such samples.

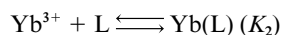
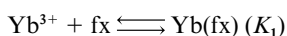
The 1:1 complex is detectable with electrospray mass spectrometry. Under the condition that excess fx is present, the typical isotope pattern for a mononuclear Yb^{3+} complex is found at m/z 792 ($\text{Yb}(\text{fx}) - \text{H}^+$). With excess Yb^{3+} this pattern disappeared, but unfortunately no other types of complexes

could be identified in these solutions under the experimental conditions, preventing a more precise characterisation of the type of 'aggregates' formed.

Based on the mass spectrometric data and the spectroscopic titration, it can be concluded that stable 1 : 1 complexes between fx and Yb³⁺ are formed provided no excess of lanthanide ions is present. All complexes for the photophysical measurements were therefore made by mixing equal amounts of equimolar solutions of ion and ligand. Formation of 1 : 1 complexes was then checked by measuring the luminescence decay curves: these should be monoexponential.

Complex stability

A way to find out about the stability of Yb(fx) is taking a solution of this complex and adding a second ligand, L, to it that also forms 1 : 1 complexes with Yb³⁺. Now fx and L have to compete for the Yb³⁺ ions. The following equilibria exist:



If ligand L forms complexes that do not luminesce upon excitation with visible light, the success of fx in the 'struggle' for Yb³⁺ is directly related to the sensitised Yb³⁺ photoluminescence intensity of the solution. In the case of an optically dilute solution, this intensity is in fact linearly proportional to the concentration of Yb(fx).

Let c_{Yb} , c_{fx} and c_{L} be the total concentrations of Yb³⁺, fluorexon and non-sensitising competing ligand, respectively. We have equal total concentrations of Yb³⁺ and fx [eqn. (1)]:

$$c_{\text{Yb}} = c_{\text{fx}} = c \quad (1)$$

The relative luminescence intensity of the solution, I , is given by eqn. (2) so that it equals 1 before L is added (provided of course

$$I = \frac{[\text{Yb}(\text{fx})]}{c} \quad (2)$$

that $c \gg 1/K_1$). After addition of L and equilibration of the solution, some Yb(fx) will have been replaced by Yb(L), resulting in a decrease of the luminescence. It can be shown that the relative stability of Yb(fx) is related to I by eqn. (3). Fig. 5 contains the

$$\frac{K_1}{K_2} = \frac{I^2 + I \left(\frac{c_{\text{L}}}{c} - 1 \right)}{I^2 - 2I + 1} \quad (3)$$

result of a typical competition experiment in which at a certain time ("A", after 755 s), 5 equivalents of EDTA are added to a solution of Yb(fx) in Tris-HCl buffer. One sees that after the addition the Yb³⁺ luminescence intensity gradually decreases (monoexponentially with a time constant of $7.1 \times 10^4 \text{ s}^{-1}$) and settles at a value 12% of that of the initial value. The rate determining step in the equilibration is probably the dissociation of Yb(fx), which is apparently quite slow indicating a high kinetic stability of the complex. The thermodynamic stability is also rather high. It is of the same order of magnitude as that of the Yb(EDTA) complex. The ratio of their equilibrium constants was calculated using eqn. (3), and amounts to 0.7.

Photophysical processes and properties

Having established that stable 1 : 1 complexes of fx with lanthanide ions can be prepared, the photophysical properties of these complexes were studied. The main photophysical processes are depicted in Fig. 6. The antenna function of the chromophore relies on it having a large absorption cross-section (extinction

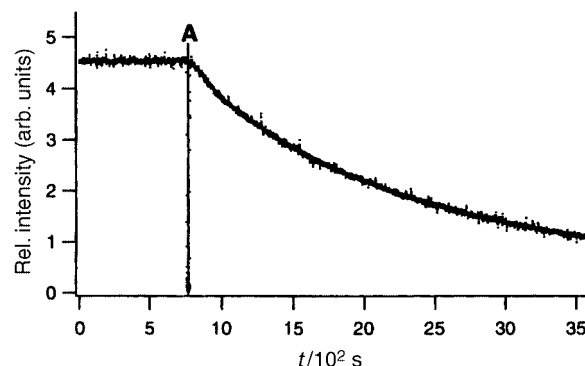


Fig. 5 NIR luminescence (excited at 480 nm, monitored at 980 nm) of a solution of Yb(fx) ($1.1 \times 10^{-5} \text{ M}$) in water. At "A" ($t = 755 \text{ s}$), five molar equivalents of EDTA were added to the solution.

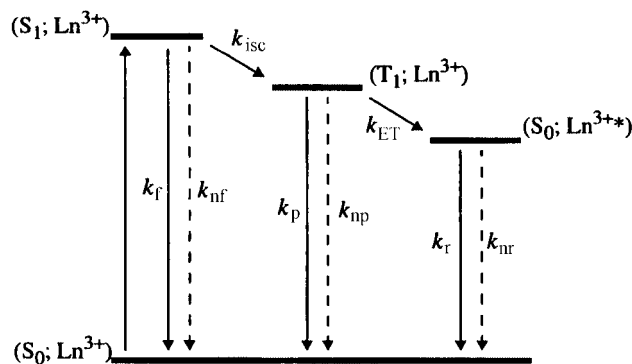


Fig. 6 Simple photophysical diagram, showing the main processes in luminescent complexes. The electronic states of the complex are indicated in the form (antenna; ion), where antenna denotes the state of the antenna chromophore and ion denotes the state of the lanthanide ion. k_{nr} , k_{r} : rates of non-radiative and radiative deactivation of the antenna singlet; k_{isc} : intersystem crossing rate; k_{np} , k_{p} : rates of non-radiative and radiative deactivation of the antenna triplet; k_{ET} : rate of energy transfer; k_{nr} , k_{r} : non-radiative and radiative rates of depopulation of the lanthanide's excited state.

coefficient) compared to the lanthanide ion. $\epsilon_{\text{antenna}}/\epsilon_{\text{ion}}$ might very well exceed 10000. Then, the antenna should waste none of the absorbed energy in a process like (antenna) fluorescence (k_{r}), but rather transfer its singlet energy directly to the lanthanide ion or undergo intersystem crossing to the triplet state (k_{isc}). The process of singlet energy transfer has never been observed experimentally, and is expected to be inefficient when it has to compete with other processes. Thus, intersystem crossing is also a necessary process. Next, the triplet energy should be transferred to the lanthanide ion as quickly as possible (k_{ET}), to prevent other deactivating processes such as phosphorescence (k_{p}) and non-radiative decay (k_{np} , including quenching by oxygen) from competing. Finally, the lanthanide ion should be efficient in emitting photons (k_{r}) instead of releasing its energy to vibrational modes in the surrounding ligand and solvent molecules (k_{nr}). We will not focus on the latter aspect, but it is known that the near-infrared emissions of Nd³⁺, Er³⁺ and Yb³⁺ are easily quenched by most common organic vibrations, such as O-H, N-H and C-H bonds,^{20,21,26-28} so one should expect the lanthanide emission step to limit the overall luminescence quantum yield.

Absorption properties. Interestingly, we discovered that the absorption spectra of the complexes are different for each lanthanide ion. Therefore, not only the spectra of the Nd³⁺, Yb³⁺ and Er³⁺ complexes were recorded but also those of Gd³⁺, Eu³⁺ and Pr³⁺ (Fig. 7). There is a correlation between the shape of the spectrum and the size of the lanthanide ion. On going from the "big" Nd³⁺ to the "small" Er³⁺ and Yb³⁺ ions, the absorption band becomes sharper with a higher maximum extinction

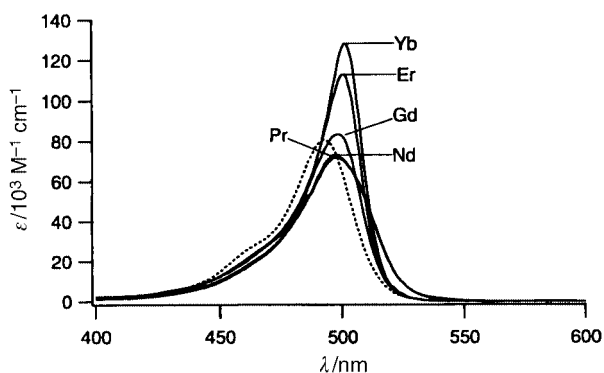


Fig. 7 Absorption spectra of fluorexon (dotted line) and its 1:1 lanthanide complexes (solid lines) in 0.1 M Tris-HCl buffer (pH 8.3).

coefficient. This behaviour contrasts with that of the AMFLU-DTPA ligand, which shows no significant changes in its absorption spectrum upon complexation with a lanthanide ion. The chromophore in fluorexon obviously senses the presence of the ion in its vicinity, indicating that the chromophore-ion distance is considerably smaller than in the corresponding AMFLU-DTPA complexes. Compared to 'free' fx, the lanthanide complexes have larger absorption cross-sections and have their maximum at slightly longer wavelengths.

Antenna fluorescence. Unlike in the AMFLU-DTPA-lanthanide complexes,¹⁴ the antenna fluorescence is effectively quenched in the fluorexon complex. The free ligand has a fluorescence quantum yield of 0.85, in the Yb³⁺ complex this is less than 0.01.‡ This is not only the case in Yb(fx), but also in Nd(fx), Er(fx), and Gd(fx). Three mechanisms may be invoked to explain the quenching: energy transfer from the singlet state of the chromophore, electron transfer and intersystem crossing. Singlet energy transfer can be ruled out: Gd³⁺ still quenches the fluorescence to the same extent as the three other ions, but has no energy levels that can receive energy from singlet excited fluorexon.

Electron transfer might only occur in the case of Yb(fx), since Yb³⁺ is quite easily reduced and xanthene dyes such as fluorexon are able to act as electron donors in their excited states.²⁹ It has been found that in contrast to the other (electrochemically inert) lanthanide ions, Yb³⁺ and Eu³⁺ quench the fluorescence of fluorophores with high singlet energies, such as tryptophan.^{30,31} Horrocks *et al.*³² claim that such redox processes may even lead to photosensitised Yb³⁺, when the energy released in subsequent charge recombination is enough to excite Yb³⁺. The fluorexon fluorescence, however, is also quenched by Nd³⁺, Gd³⁺ and Er³⁺. Therefore, we expect that electron transfer quenching does not play a role. This expectation is supported by the fact that neither Yb³⁺ nor Eu³⁺ quenches the fluorescence of the chromophore in AMFLU-DTPA to a larger extent than other lanthanide ions do.^{14,15}

Thus, enhancement of the intersystem crossing due to the paramagnetic and heavy atom effects is the most likely cause of the fluorescence quenching. Compared to AMFLU-DTPA complexes the effect in the fluorexon systems is much more pronounced, again a result of the smaller distance between chromophore and lanthanide ion. On the basis of the complete quenching of antenna fluorescence, k_{isc} can be estimated to be $>10^{10} \text{ s}^{-1}$.

Triplet state. Also in Gd(fx) the fluorexon fluorescence is almost totally quenched, which can only be due to enhancement of intersystem crossing. Gd³⁺ is electrochemically inactive and has no energy levels below 32200 cm⁻¹, preventing it from

‡ The excitation spectrum of the residual fluorescence reveals that it probably stems from a minor impurity, fluorescein.

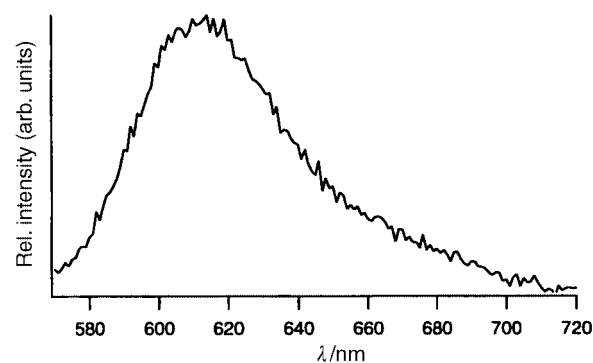


Fig. 8 Phosphorescence of Gd(fx) in water at room-temperature, excited at 500 nm and detected using delayed detection.

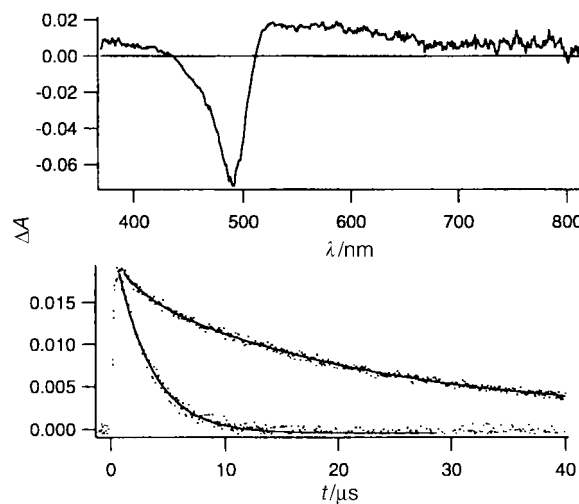


Fig. 9 Transient absorption spectroscopy of Gd(fx) in Tris-HCl buffer. Top: transient absorption spectrum of Gd(fx), recorded 100 ns after the laser pulse. The bleaching around 495 nm is due to depopulation of the ground state of Gd(fx). The ligand centered triplet-triplet absorption of the complex is a broad band that peaks at 530 nm. Bottom: time-resolved transient absorption of the (T₁; Gd³⁺) state, monitored at 530 nm.

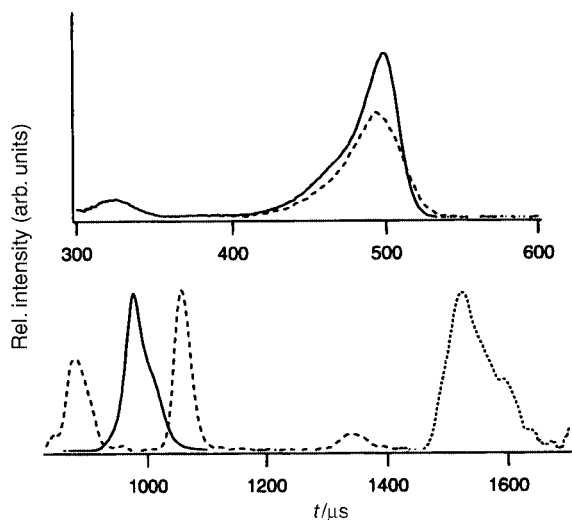
quenching the singlet state of fluorexon by electron transfer or singlet energy transfer. Moreover, the lack of accepting levels makes the Gd³⁺ complex suitable for having a look at the triplet state of the antenna chromophore. In deoxygenated solution, even at room temperature, phosphorescence of Gd(fx) is readily observed by using gated detection: equipping the fluorimeter with a rotating drum to introduce a delay between excitation and detection yields the phosphorescence spectrum shown in Fig. 8 (solid line).

Also transient absorbance measurements at room temperature reveal efficient formation of a triplet state. Whereas free ligand fluorexon and Yb(fx), Nd(fx), Er(fx) show no long-lived (>20 ns) excited state absorptions under the experimental conditions, Gd(fx) displays the transient absorption spectrum in Fig. 9 (top). Fig. 9 (bottom) shows the corresponding single-wavelength decays at 530 nm, in deoxygenated and aerated solution. In aerated solution the triplet lives 3.1 μs, this lifetime increases to 21 μs in deoxygenated buffer.

The heavy atom induced formation of fluorexon triplet states implies that Gd(fx) is an able sensitiser of singlet oxygen. Interaction of triplet molecular oxygen with triplet states produces singlet oxygen, which we monitor by its phosphorescence at 1276 nm. In buffered air-equilibrated D₂O the formation of singlet oxygen by excited Gd(fx) is almost as efficient as that observed with eosin. The Yb³⁺, Nd³⁺, Er³⁺ complexes of fluorexon show no singlet oxygen signal at all, whereas the corresponding AMFLU-DTPA complexes produce fair amounts of singlet oxygen upon excitation.¹³

Table 1 Observed luminescence lifetimes, τ_{obs} , and estimates for the quantum yield of the lanthanide photoluminescence step, $\Phi_{\text{Ln}}^{\text{est}}$

Ln(fx)	H ₂ O		D ₂ O	
	$\tau_{\text{obs}}/\mu\text{s}$	$\Phi_{\text{Ln}}^{\text{est}}$	$\tau_{\text{obs}}/\mu\text{s}$	$\Phi_{\text{Ln}}^{\text{est}}$
Yb ³⁺	1.91	1×10^{-3}	10.4	5×10^{-3}
Nd ³⁺	0.25	3×10^{-4}	0.58	7×10^{-4}
Er ³⁺	—	—	1.46	2×10^{-4}

**Fig. 10** Luminescence spectra of near-infrared luminescent Ln(fx) complexes in D₂O (buffered with deuterated Tris, pD 8.3). Top: Excitation spectra of Yb(fx) (emission monitored at 980 nm) and Nd(fx) (1060 nm). Bottom: Emission spectra (excitation 480 nm) of Nd(fx) (dashed line), Yb(fx) (solid line) and Er(fx) (dotted line).

Luminescence. Excitation of the corresponding complexes of fluorexon leads to near-infrared luminescence of Yb³⁺ (²F_{7/2} → ²F_{5/2}, 980 nm), Nd³⁺ (main band is at 1060 nm, ⁴F_{3/2} → ⁴I_{11/2}) or Er³⁺ (⁴I_{13/2} → ⁴I_{11/2}, 1530 nm) (Fig. 10). The structure on the single emission lines of the lanthanide ions is due to crystal field splitting of the degenerate *J* levels.

The excitation spectra of lanthanide luminescence match the absorption spectra. Interestingly, the overall quantum yield of this luminescence is virtually independent of the oxygen concentration. In contrast to our earlier observations for NIR emitting lanthanide complexes of AMFLU-DTPA oxygenation did not decrease the luminescence intensity. Therefore not only intersystem crossing is fast and efficient, but also the transfer of triplet energy to the lanthanide ion, since oxygen cannot compete as an alternative acceptor.

This is also apparent from time-resolved luminescence measurements (Table 1). Whereas the luminescence of Yb(AMFLU-DTPA) and that of Er(AMFLU-DTPA) in deoxygenated D₂O show biexponential behaviour having both a rising and a decaying component on the microsecond timescale due to slow energy transfer,¹⁵ all fx complexes show monoexponential decay. Slow energy transfer would result in a rising component in the time-resolved luminescence, but clearly the formation of the lanthanide excited state in the Ln(fx) complexes (which includes the energy transfer) occurs within the time resolution of the measurement (≤100 ns).

The luminescence lifetimes are in line with what is usually observed for the three near-infrared emitting ions encapsulated in organic ligands.^{20,21,28,33,34} Nonradiative deactivation of the luminescent state is efficient, since it can be effectively mediated by the ubiquitous molecular vibrations, as already mentioned.

Overall luminescence quantum yield. That non-radiative deactivation of the luminescent state is indeed efficient is seen from the quantum yields in Table 2. Each of these “overall”

Table 2 Observed overall NIR luminescence quantum yields upon ligand excitation, Φ_{tot} , and estimated sensitisation efficiencies, $\eta_{\text{sens}}^{\text{est}}$

Ln(fx)	H ₂ O		D ₂ O	
	Φ_{tot}	$\eta_{\text{sens}}^{\text{est}}$	Φ_{tot}	$\eta_{\text{sens}}^{\text{est}}$
Yb ³⁺	8.9×10^{-4}	0.9	4.5×10^{-3}	0.9
Nd ³⁺	1.7×10^{-4}	0.5	3.8×10^{-4}	0.5
Er ³⁺	^a		1.9×10^{-4}	1.0

^a Er³⁺ shows no detectable luminescence in H₂O, because H₂O has strong absorptions in the 1500 nm range.

luminescence quantum yields (Φ_{tot}) is the product of the yields of the three steps involved in producing photoluminescence: intersystem crossing (Φ_{ISC}), energy transfer (Φ_{ET}) and lanthanide luminescence (Φ_{Ln}) [eqn. (4)]. The quantum yield of

$$\Phi_{\text{tot}} = \Phi_{\text{ISC}}\Phi_{\text{ET}}\Phi_{\text{Ln}} \quad (4)$$

the lanthanide luminescence step can be calculated from the observed luminescence lifetime (τ_{obs}), if the radiative (or “natural”) lifetime τ_{rad} is known [eqn. (5)]. Estimates of τ_{rad} in

$$\Phi_{\text{Ln}} = \frac{\tau_{\text{obs}}}{\tau_{\text{rad}}} \quad (5)$$

organic systems are 8 ms, 2 ms and 0.8 ms, for Er³⁺, Yb³⁺ and Nd³⁺, respectively.^{14,15} The values of Φ_{Ln} calculated on the basis of eqn. (5) and these estimates have been tabulated in Table 1. These values of Φ_{Ln} enable us to estimate the sensitisation efficiency, η_{sens} , given by eqn. (6).

$$\eta_{\text{sens}} = \Phi_{\text{ISC}}\Phi_{\text{ET}} \quad (6)$$

The calculated efficiencies collected in Table 2 demonstrate that sensitisation of NIR lanthanide photoluminescence in the fluorexon complexes is indeed an efficient process.

Conclusion

Fluorexon forms water-soluble 1:1 complexes with lanthanide ions. These complexes have a high kinetic stability and a thermodynamic stability that is approximately equal to the corresponding EDTA complexes. Enhanced sensitisation of Yb³⁺ (980 nm), Nd³⁺ (main transition at 1060 nm) and Er³⁺ (1530 nm) has been achieved compared to the former “generation” of complexes. The sensitisation efficiency is determined by Φ_{ISC} and Φ_{ET} , and both these factors benefit from the shortened distance in the present fluorexon–lanthanide ion system.

This result once again points out the superiority of complexes that have the antenna chromophore and lanthanide binding site integrated over complexes in which these have been introduced as separate units. An example is the triphenylenes which are much less effective antenna chromophores when attached to a calixarene ionophore¹¹ than when being the complexing moiety themselves.³⁵

Another fact demonstrated by the fluorexon–near-infrared emitting lanthanide ion system is that a fluorescent chromophore is not necessarily a bad antenna for lanthanide ions. High radiative rates for fluorescence imply large absorption cross-sections and high fluorescence quantum yields indicate the absence of non-radiative deactivation. If the lanthanide ion is close enough to enhance intersystem crossing in a chromophore by heavy atom and paramagnetic effects, an initially highly fluorescent chromophore may become a powerful sensitiser of lanthanide luminescence.

The ability of Gd³⁺ to increase intersystem crossing and the radiative rate of phosphorescence of fluorexon is demonstrated by the presence of room-temperature phosphorescence, long-

lived triplet–triplet absorption and generation of singlet oxygen. This appears to be a relatively unexplored and unexploited area of the photophysical properties of lanthanide complexes containing organic chromophores. Enhanced singlet oxygen generation by chromophores in Gd³⁺ complexes may have medical use, e.g. in photodynamic therapy.

The fluorexon ligand might be fitted with a reactive group so that it can be attached to biological molecules (proteins, nucleotides). It is then possible to construct near-infrared luminescent probes for fluorimmunoassays and fluorescence microscopy. In these applications, the advantages of long-lived, near-infrared luminescence excited with visible light may very well outweigh the low luminescence quantum yields.

Acknowledgements

The authors are very grateful to Michel Nielen (Akzo Nobel Central Research) for recording and discussing the electrospray mass spectra. John van Ramesdonk is acknowledged for his skilful assistance in setting up the spectrograph/CCD and transient absorption instruments. Akzo Nobel Central Research is acknowledged for financial and technical support.

References

- 1 M. P. Bailey, B. F. Rocks and C. Riley, *Analyst (London)*, 1984, **109**, 1449.
- 2 E. Soini and T. Lövgren, *CRC Crit. Rev. Anal. Chem.*, 1987, **18**, 105.
- 3 G. Mathis, *Clin. Chem.*, 1993, **39**, 1953.
- 4 J. Coates, P. G. Sammes, G. Yahioğlu, R. M. West and A. J. Garman, *J. Chem. Soc., Chem. Commun.*, 1994, 2311.
- 5 I. Hemmilä, *J. Alloys Compd.*, 1995, **225**, 480.
- 6 M. P. Houlne, T. S. Agent, G. E. Kiefer, K. McMillan and D. J. Bornhop, *Appl. Spectrosc.*, 1996, **50**, 1221.
- 7 R. R. De Haas, N. P. Verwoerd, M. P. Van der Corput, R. P. Van Gijlswijk, H. Siitari and H. J. Tanke, *J. Histochem. Cytochem.*, 1996, **44**, 1091.
- 8 S. I. Weissman, *J. Chem. Phys.*, 1942, **10**, 214.
- 9 G. A. Crosby, R. E. Whan and R. M. Alire, *J. Chem. Phys.*, 1961, **34**, 743.
- 10 J. H. Van Vleck, *J. Chem. Phys.*, 1937, **41**, 67.
- 11 F. J. Steemers, W. Verboom, D. N. Reinhoudt, E. B. Van der Tol and J. W. Verhoeven, *J. Am. Chem. Soc.*, 1995, **117**, 9408.
- 12 M. H. V. Werts, M. A. Duin, J. W. Hofstraat and J. W. Verhoeven, *Chem. Commun.*, 1999, 799.
- 13 M. H. V. Werts, J. W. Hofstraat, F. A. J. Geurts and J. W. Verhoeven, *Chem. Phys. Lett.*, 1997, **276**, 196.
- 14 J. W. Hofstraat, M. P. Oude Wolbers, F. C. J. M. van Veggel, D. N. Reinhoudt, M. H. V. Werts and J. W. Verhoeven, *J. Fluoresc.*, 1998, **8**, 301.
- 15 M. H. V. Werts, unpublished work.
- 16 W. M. F. Fabian, S. Schuppler and O. S. Wolfbeis, *J. Chem. Soc., Perkin Trans. 2*, 1996, 853.
- 17 J. Shi, X. Zhang and D. C. Neckers, *J. Org. Chem.*, 1992, **57**, 4418.
- 18 J. Shi, X. Zhang and D. C. Neckers, *Tetrahedron Lett.*, 1993, **34**, 6013.
- 19 S. Tobita, M. Arakawa and I. Tanaka, *J. Phys. Chem.*, 1985, **89**, 5649.
- 20 A. Beeby and S. Faulkner, *Chem. Phys. Lett.*, 1997, **266**, 116.
- 21 A. Beeby, R. S. Dickens, S. Faulkner, D. Parker and J. A. G. Williams, *Chem. Commun.*, 1997, 1401.
- 22 J. Van Houten and R. J. Watts, *J. Am. Chem. Soc.*, 1976, **98**, 4853.
- 23 J. N. Demas and G. A. Crosby, *J. Phys. Chem.*, 1971, **75**, 991.
- 24 D. F. Eaton, *J. Photochem. Photobiol. B*, 1988, **2**, 523.
- 25 D. Magde, J. H. Brannon, T. L. Cremers and J. Olmsted III, *J. Phys. Chem.*, 1979, **83**, 696.
- 26 G. Stein and E. Würzberg, *J. Chem. Phys.*, 1974, **62**, 208.
- 27 Y. Hasegawa, Y. Kimura, K. Murakoshi, Y. Wada, J.-H. Kim, N. Nakashima, T. Yamanaka and S. Yanagida, *J. Phys. Chem.*, 1996, **100**, 10201.
- 28 M. P. Oude Wolbers, F. C. J. M. van Veggel, B. H. M. Snellink-Ruël, J. W. Hofstraat, F. A. J. Geurts and D. N. Reinhoudt, *J. Chem. Soc., Perkin Trans. 2*, 1998, 2141.
- 29 D. C. Neckers and O. M. Valdes-Aguilera, *Adv. Photochem.*, 1993, **18**, 315.
- 30 A. Abusaleh and C. F. Meares, *Photochem. Photobiol.*, 1984, **39**, 763.
- 31 W. B. Kirk, W. S. Wessels and F. G. Prendergast, *J. Phys. Chem.*, 1993, **97**, 10326.
- 32 W. D. Horrocks, Jr., J. P. Bolender, W. D. Smith and R. M. Supkowski, *J. Am. Chem. Soc.*, 1997, **119**, 5972.
- 33 N. V. Rusakova, S. B. Meshkova, V. Y. Venchikov, V. E. Pyatosin and M. P. Tsvirko, *J. Appl. Spectrosc.*, 1992, **56**, 488.
- 34 M. A. Pavier, T. Richardson, T. M. Searle, C. H. Huang, H. Li and D. Zhou, *Supramol. Sci.*, 1997, **4**, 437.
- 35 E. B. van der Tol, H. J. van Ramesdonk, J. W. Verhoeven, F. J. Steemers, E. G. Kerver, W. Verboom and D. N. Reinhoudt, *Chem. Eur. J.*, 1998, **4**, 2315.

Paper a909662k

